engineering proceedings

MDPI

Proceeding Paper

PV Energy Prediction in 24 h Horizon Using Modular Models Based on Polynomial Conversion of the L-Transform PDE Derivatives in Node-by-Node-Evolved Binary-Tree Networks †

Ladislav Zjavka * and Václav Snášel

Department of Computer Science, Faculty of Electrical Engineering and Computer Science, VŠB-Technical University of Ostrava, 708 00 Ostrava, Czech Republic; vaclav.snasel@vsb.cz

* Correspondence: ladislav.zjavka@vsb.cz

† Presented at the 8th International Conference on Time Series and Forecasting, Gran Canaria, Spain, 27–30 June 2022.

Abstract: Accurate daily photovoltaic (PV) power predictions are challenging as near-ground atmospheric processes include complicated chaotic interactions among local factors (ground temperature, cloudiness structure, humidity, visibility factor, etc.). Fluctuations in solar irradiance resulting from the cloud structure dynamics are influenced by many uncertain parameters, which can be described by differential equations. Recent artificial intelligence (AI) computational tools allow us to transform and post-validate forecast data from numerical weather prediction (NWP) systems to estimate PV power generation in relation to on-site local specifics. However, local NWP models are usually produced each six hours to simulate the progress of main weather quantities in a medium-scale target area. Their delay usually covers several hours, further increasing the inadequate operational quality required in PV plants. All-day prediction models perform better, if they are developed with the last historical weather and PV data. Differential polynomial neural network (D-PNN) is a recently designed computational method, based on a new learning approach, which allows us to represent complicated data relations contained in local weather patterns to account for irregular phenomena. D-PNN combines two-input variables to split the partial differential equation (PDE), defined in the general order k and n variables, into partition elements of two-input node PDEs of recognized order and type. The node-determined sub-PDEs can be easily converted using operator calculus (OC), in several types of predefined convert schemes, to define unknown node functions expressed in the Laplace images form Application of the inverse L-transformation formula to the L-converts results in obtaining the prime function originals. D-PNN elicits a progressive modular tree structure to assess one-by-one the optimal PDE node solutions to be inserted in the sum output of the overall expanded computing model. Statistical modular models are the result of learning schemes of preadjusted day data records from various observational localities. They are applied after testing to the rest of unseen daily series of known data to compute estimations of clear-sky index (CSI) in the 24 h input-delayed time-sequences.

Keywords: modelling dynamics; differential learning; multinomial tree; operator calculus; conversion scheme; Laplace image

Citation: Zjavka, L.; Snášel, V. PV Energy Prediction in 24 h Horizon Using Modular Models Based on Polynomial Conversion of the L-Transform PDE Derivatives in Node-by-Node-Evolved Binary-Tree Networks. *Eng. Proc.* **2022**, *18*, 34. https://doi.org/10.3390/engproc2022018034

Academic Editors: Ignacio Rojas, Hector Pomares, Olga Valenzuela, Fernando Rojas and Luis Javier Herrera

Published: 27 June 2022

1. Introduction

Stochastic photovoltaic power (PVP) production can hardly be predicted when relying solely on NWP data units, which cannot fully account for local anomalies in the near-ground surface terrain [1]. NWP utilities try to integrate their output with sky- or ground-produced image data patterns to localize and identify the development of cloud structure formations on a regional scale [2]. Middle-time horizon NWP forecasting can be fused with clear sky data modelling and re-analyzed to determine the optimal interval sizes of training samples.

Distribution data based on forecast errors, obtained for various cloudiness situations, can be used to define probability intervals in prediction days and to represent inhomogeneous weather states. An increase in the modular temperature of photovoltaic panels results in a decrease in efficient power production and irradiance conversion [3]. AI computing is not focused on the direct recognition of particular physical development on multilayer atmosphere scales. They usually use the available size of data records in modelling or analyzing local atmospheric progress. Statistics can be applied in short-time prediction of, or need to fuse combine their data processing with, NWP forecasting in a larger day horizon. Irradiance inputs and target PVP output sequences in a day-determined range can be used in statistical analyses or AI learning. The statistics models were applied to 24–48 h middle-scale data to post-process the system forecasts and compute PVP at all input–output-related sequence times. The conversion of NWP data has some drawbacks; the model functionality shows a great dependency on the applicability and reliability of the forecast data in processing [4]. The quality of AI-based learning predictions can essentially differ; the statistical procedure must undergo appropriate initialization and testing. Many AI methods show some limitations, for example, model unfitting or inadequate generalization related to local constraints of PVP plant designs. AI solutions can process additional data features or use extra units (cloudiness motion, spectral analysis) to recognize character of fluctuations or type structures in cloudiness formation processes. Popular hybrid techniques fuse different computing or processing approaches, additionally combining the unique key-model features to innovate the inadequate performance. Multistep forecasting can be direct or iterative (or a combination). In the first, the values are forecasted all at once at different times, contrary to the second approach, where iteratively predicted data at the previous time steps are supplied for the input vectors at the following computing time sequences. Additional solar features can be used, e.g., clearness factor, cloudiness index, aerosol and visibility parameter, turbidity, sun angle, or azimuth. The summation ensembles form a weighted model output to compute the final result according to the predetermined weather type or probabilistic reliability. If single-model forecasts differ in a large measure, the overall output is given a significant uncertainty. In contrast, when the results of the ensemble models show a large similarity, the uncertain character of the output model is greatly reduced. Probability intervals in the model output define an uncertainty range in computing reliable data estimations under different initial constraint statistics density.

The new differential learning is used to gradually elicit structures based on the form of a polynomial neural network (PNN), initially using one node, to partition and transform the general PDE of n variables into summation modules of single PDEs in blocks of two-variable nodes. The rational components are obtained in the form of Laplace transform images of unknown node functions, formed according to operator calculus (OC) procedures [5]. The inverse L-operation is applied to the node-produced rational components, based on the OC expression. Unknown node originals are obtained to be summed in the overall output of the n-variable PDE model. D-PNN combines and extracts the most applicable node input couples in each layer, step by step, to generate modular subcomponents from the originally defined PDEs and extend with them the iterative solution to reach the output error minima. The appropriate testing procedure can employ the external complement scheme to allow adaptation and adjustment of those node components, minimizing all computed errors in training and testing defined by the modelling constraint of a problem [6]. Historical observations with 24 h delay between input and output data are processed to pre-assess the optimal lengths of daily intervals, which enable us to obtain the operable statistics predictions in a day horizon. Finally, the tested models can compute their output sequences in the defined time horizon in relation to the processed last-day input data and the learned patterns included in the determined data sample range.

2. 24 h Sequenced PV-Output Prediction Based on Data Record Statistics

AI regression was used in training the 24 h delay between input–output data patterns (blue, left), selected in the optimal day-range sequences, by the initial assessment model.

The statistic models were developed in multisite data processing to apply the last known observation input series to forecast the complete day light cycle of PV power production in the applied 24 h trained prediction horizon (red, right). PVP production in the next 24 h is calculated by processing series at the related times in sequence data in the previous day. Initial assessment models examine data intervals, gradually increasing their days, to pre-define the optimal training process. Their computed output is compared one by one with the time-related data of the target CSI in the reserved part, to obtain the best accuracy. Error minima determine the approximate number of applicable day records that can be used in training. The recognized day-data patterns show mostly a degree of similarity compared to the latest observational hours used in the final testing. This procedure can successfully obtain up-to-date models that can process the unknown last-day input series (Figure 1) in most day-experiment instances.

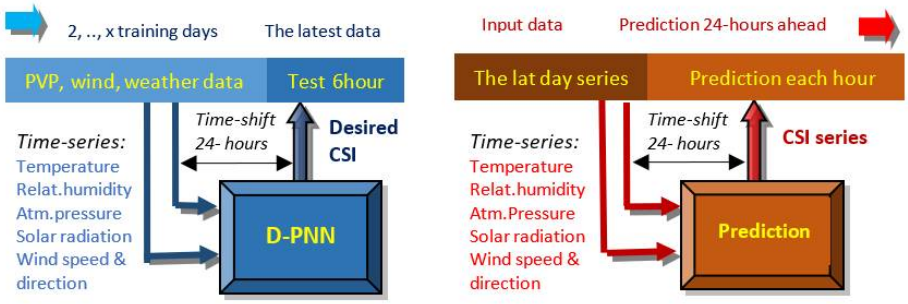

Figure 1. CSI day-sequence forecasting by models (red **right**) resulting from training for the initially assessed day-data patterns in an all-day input–output horizon (blue **left**).

The clear-sky index (CSI) is a relative solar parameter defined by ratio of the real to the ideal PVP considering total clear sky at any day time cycles. It is necessary to compute the output of the model in training and prediction [7] regardless of changes in the actual values, directly related to the PVP cycles in a time. PVP pattern change considerably as a result of different atmospheric conditions and local anomalies (e.g., cloudiness type, humidity character, wind gusts, etc. Overnight sudden changes in the previous pattern can cause difficulties in training. The statistically developed model may be completely out of date, unable to process unrecognized data series in prediction. NWP processing data can be applied in these sudden cases [5]. Figure 2 shows the frontal change in PVP patterns on 3 May.

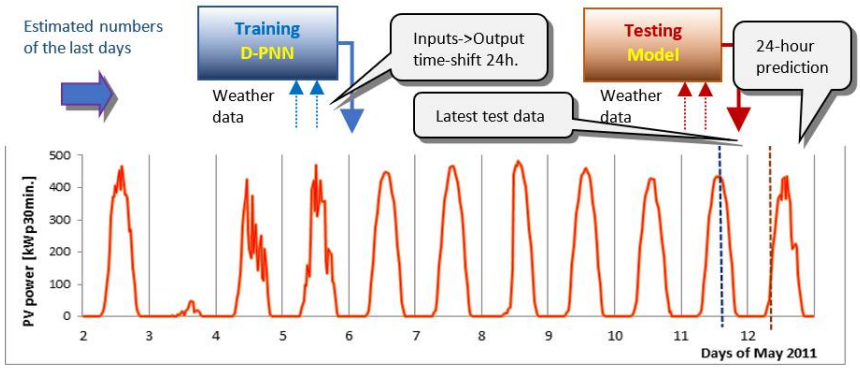

Figure 2. Model development, testing and CSI final output computing (red, right) related to changing PVP day patterns in the fixed 24 h input–output time delay (blue, left).

3. PDE Conversion and L-Transformation Using Operator Calculus

D-PNN evolves binary-tree structures to partition the generally defined PDE of n variables into determined-order sub-PDEs of two variables (using data samples). The

simple PDEs are L-transformed using OC definitions into rational components, forming the Laplace images for the node-searched unavailable summation term series. Inverse members determined by L-restoration are used to calculate the overall output to model the separable function of n variables, initially defined only by the PDE [8].

$$a + bu + \sum_{i=1}^{n} c_i \frac{\partial u}{\partial x_i} + \sum_{i=1}^{n} \sum_{j=1}^{n} d_{ij} \frac{\partial^2 u}{\partial x_i \partial x_j} + ... = 0 \quad (1)$$

$$u = \sum_{k=1}^{\infty} u_k \quad (2)$$

where the following are defined: $u(x_1, x_2, \ldots, x_n)$—unknown separable function of n-input variables; a, b, c_i, d_{ij},...—weights of terms; u_i—partial sum functions.

The general form of PDE (1) can be used to describe a problem-separable u function of n inputs, which can be formulated as a non-limited convergent series (2) of simplified functions u_k of two variables initially defined by sub-PDEs (3) in an equality of eight variables.

$$F\left(x_1, x_2, u, \frac{\partial u}{\partial x_1}, \frac{\partial u}{\partial x_2}, \frac{\partial^2 u}{\partial x_1^2}, \frac{\partial^2 u}{\partial x_1 \partial x_2}, \frac{\partial^2 u}{\partial x_2^2}\right) = 0 \quad (3)$$

where u_k are node partial sum functions of an unknown separable function u.

The adapted polynomial conversion using OC formulas for the derivatives $f(t)$ described by an ordinary differential equation (ODE) is based on the proposition that the Laplace transformation is applicable in the case of known initial conditions (4).

$$L\left\{ f^{(n)}(t) \right\} = p^n F(p) - \sum_{k=1}^{n} p^{n-i} f_{0+}^{(i-1)} \quad L\{ f(t) \} = F(p) \quad (4)$$

where the following are defined: $f(t), f'(t), \ldots, f^{(n)}(t)$—originals continuous in <0+, ∞>; p, t—complex and real variables.

Polynomial conversion applied to ODE derivatives results in a set of Equation (4), where the Laplace transform $F(p)$ can be formulated through the complex conjugate p. $F(p)$ is separated in a rational term (5) to define the L-image of the function $f(t)$. The inverse transform of OC of the ration term restores the original $f(t)$ of a real variable t (5).

$$F(p) = \frac{P(p)}{Q(p)} = \frac{Bp + C}{p^2 + ap + b} = \sum_{k=1}^{n} \frac{A_k}{p - \alpha_k} \quad (5)$$

where the following are defined: B, C, A_k—coefficients of elementary fractions; a,b—polynomial parameters.

$$F(p) = \frac{P(p)}{Q(p)} = \sum_{k=1}^{n} \frac{P(\alpha_k)}{Q_k(\alpha_k)} \frac{1}{p - \alpha_k} \qquad f(t) = \sum_{k=1}^{n} \frac{P(\alpha_k)}{Q_k(\alpha_k)} e^{\alpha_k \cdot t} \quad (6)$$

where the following are defined: α_k—simple real roots of the multinomial; $Q(p)$, $F(p)$—L-transform image.

Rational components (8), formed to express the Laplace image terms of u_k functions (2), which are not available, result from the GMDH polynomials (7) composed of binary nodes of a PNN tree structure (Figure 3) in the PDE converting procedure. The inverse L operation is necessary (8) in the PNN nodes according to the definition of OC (6). The sum of originals determined by binary nodes in the partial u_k is used to calculate the overall model u (2) [8]. Each D-PNN node, using the GMDH output, groups possible simple or composite member solutions (8) for specific two-input sub-PDEs. The selected components are included in the D-PNN output sum to better converge to the target output.

$$y = a_0 + a_1 x_i + a_2 x_j + a_3 x_i x_j + a_4 {x_i}^2 + a_5 {x_j}^2 \quad (7)$$

where the following are defined: x_i, x_j—two input variables of neuron nodes.

$$y_i = w_i \frac{b_0 + b_1 x_1 + b_2 sig(x_1^2) + b_3 x_2 + b_4 sig(x_2^2)}{a_0 + a_1 x_1 + a_2 x_2 + a_3 x_1 x_2 + a_4 sig(x_1^2) + a_5 sig(x_2^2)} \cdot e^{\varphi} \tag{8}$$

where the following are defined: φ = arctg(x_1/x_2)—phase representation of two input variables; x_1, x_2, a_i, b_i—polynomial parameters; w_i—weights; *sig*—sigmoidal transform.

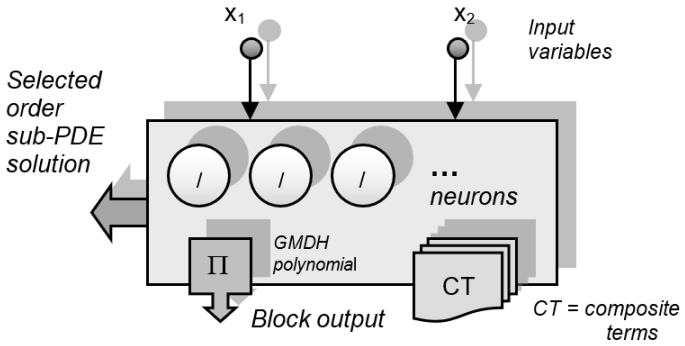

Figure 3. Block nodes of produce and group simple (/) and composite PDE member solutions.

The Euler formulation of conjugates in complex form (9), represents the conversion $f(t)$ in OC (6). The radius r is defined as a rational element, while the angle (arctg(x_2/x_1)) of two real inputs is related to the inverse restoration L of $F(p)$.

$$p = \underbrace{x_1}_{\text{Re}} + i \cdot \underbrace{x_2}_{\text{Im}} = \sqrt{x_1^2 + x_2^2} \cdot e^{i \cdot \arctan\left(\frac{x_2}{x_1}\right)} = r \cdot e^{i \cdot \varphi} = r \cdot (\cos\varphi + i \cdot \sin\varphi) \tag{9}$$

4. PDE Partition in Backward Tree Structures of D-PNN Layers

D-PNN forms progressive binary-tree structures, using composite processing functions (7) in PNN nodes, by extending/modifying the last added/processed layer with selected blocks nodes, one by one. Node blocks in secondary subsequent tree layers can form composite term (CT) products, in addition to one-fraction neurons (8). CTs are products consisting of adjustable neurons, i.e., sub-PDE converts, selected in the back-attached production blocks in the backward linked tree structure layers (Figure 4). CTs represent composite sub-PDE solutions for the node-unavailable u_k function series in the form of a product that includes images of external and internal functions commonly expressed by the derivation rules (11).

$$F(x_1, x_2, \ldots, x_n) = f(z_1, z_2, \ldots, z_m) = f(\phi_1(X), \phi_2(X), \ldots, \phi_m(X)) \tag{10}$$

$$\frac{\partial F}{\partial x_k} = \sum_{i=1}^{m} \frac{\partial f(z_1, z_2, ..., z_m)}{\partial z_i} \cdot \frac{\partial \phi_i(X)}{\partial x_k} \; k = 1, \ldots, n \tag{11}$$

For example, a block in the third layer can form additional CTs using products of sub-PDE ratio converts (12), that is, the simple neuron images of two and four back-linked tree blocks in the previous two layers (Figure 4).

$$y_{31} = w_{31} \cdot \frac{b_0 + b_1 x_{21} + b_2 x_{21}^2 + b_3 x_{22} + b_4 x_{22}^2}{a_0 + a_1 x_{21} + a_2 x_{22} + a_3 x_{21} x_{22} + a_4 x_{21}^2 + a_5 x_{22}^2} \cdot \frac{b_0 + b_1 x_{12} + b_2 x_{12}^2}{a_0 + a_1 x_{11} + a_2 x_{12} + a_3 x_{11} x_{12} + a_4 x_{11}^2 + a_5 x_{12}^2} \cdot \frac{P_{12}(x_1, x_2)}{Q_{12}(x_1, x_2)} \cdot e^{\varphi_{31}} \tag{12}$$

where the following are defined: Q_{ij}, P_{ij} = output and reduced multi-nomial of n and $n-1th$ degree; y_{kp}—pth Composite Term (CT); φ_{21} = arctg(x_{11}/x_{13}); φ_{31} = arctg(x_{21}/x_{22})φ.

The number of possible CT combinations in blocks doubles along with each back-joined preceding layer (Figure 4). Neurons in each next layer can produce more composite partial model components, using the block node outputs and PDE converts.

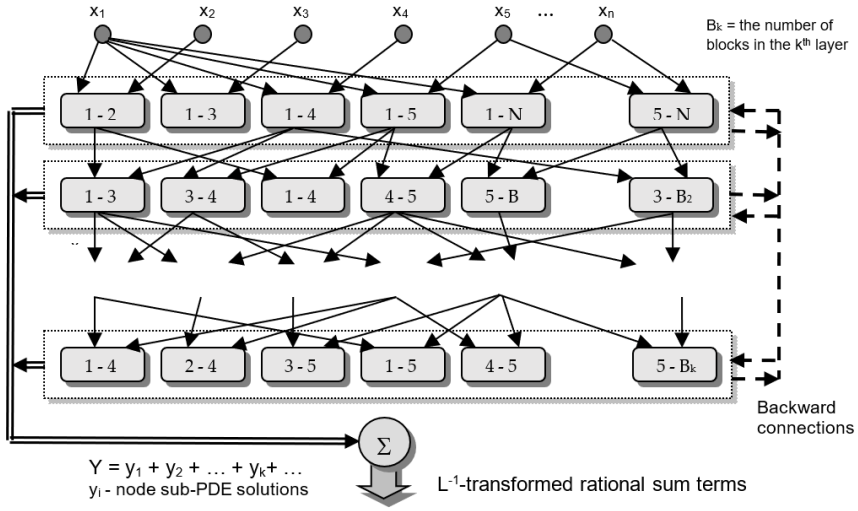

Figure 4. D-PNN searches for the most valuable input couple node blocks to generate sum PDE components, neurons and CTs, possible to insert in the overall model.

The summation model output Y is the arithmetic mean of active neurons + CT, produced in node blocks, which optimizes the adjustment and selection of PDE terms (13).

$$Y = \frac{1}{k}\sum_{i=1}^{k} y_i \tag{13}$$

where k = the number of active neurons or CTs (node PDE solutions).

Multi-objective models based on procedures can be used to optimize performance of the back-production of selected neurons and CTs in the tree-like block structure (Figure 4).

D-PNN searches for the most relevant combination couples in each input layer, analogously to the principles of GMDH [6], to form and rearrange adequate PDE components acceptable by the model. Polynomial coefficients and weights of terms are partially optimized using the gradient method [9] in each iteration tree cycle. The algorithm randomly skips the block nodes, one by one, to select and update the applied neurons or CTs involved in the complete model. The training error is calculated in relation to a continuously performed test based on the external complement restraint evaluation. This approach allows only inserting or adapting PDE components that comply with the testing restrictions. The root mean squared error (RMSE) is a gradually minimized measure of the model approximation ability at each step of training (Figure 1).

5. PVP Prediction Using the AI Pre-Determined Training Sequences in 24 h Horizon

PVP was forecasted at the Starojcka Lhota plant located in the North-East Moravian region of the Czech Republic, using historical measurements of ground environment temperature, PVP, and irradiance along with multisite spatial meteorological data of wind parameters from three nearby regional wind farms located in Maletin, Drahany, and Veseli nad Moravou. These data sets were supplied with free access airport weather observations (avg. ground temperature, avg. humidity, avg. atm. pressure, avg. wind parameters and visibility conditions) of two ground-based stations located in Brno-Turany and Ostrava-Monov (Figure 5). These standard variables were used in the development of models to predict the complete day-ahead PVP cycle data in the 24 h input–output delay. Detailed minute power measurements of the PV plant and wind farms were averaged and extrapolated to correspond to a half-hour meteorological data series from airport weather observation stations [10].

Figure 5. PVP plant and wind farm allocation in measurements and meteo-observations.

Figure 6 shows PVP forecast results of the D-PNN, Statistics and Machine Learning Tool-Box (SMLT) for Matlab regression [11], and persistent models in the 24 h horizon in specific demonstration days of the examined 2-week interval from 12–25 May 2011. The SMLT day-ahead final forecasting models were chosen considering their test error minima, obtained from the reserved part of available set data. The optimal training days, including applicable data patterns, were predetermined initially by examination of data in the previous gradually increasing training-day intervals, using a simplified model form, the same as using D-PNN (Figure 1). The SMLT forecast models resulting from Gaussian Process Regression (GPR), Support Vector Machine (SVM), and Ensemble Boosted/Bagged Tree (EBT), using the same input–output data sample variables in the next day 24 h CSI sequence prediction, obtained with the testing RMSE minima which differ only in a slight measure. Persistent comparative models, average CSI in processing series over the determined number of the last-day intervals, were used to estimate the approximation series at the responding PVP cycle day time. These oversimplified forecast benchmark solutions could be considered as daily error-reference minima.

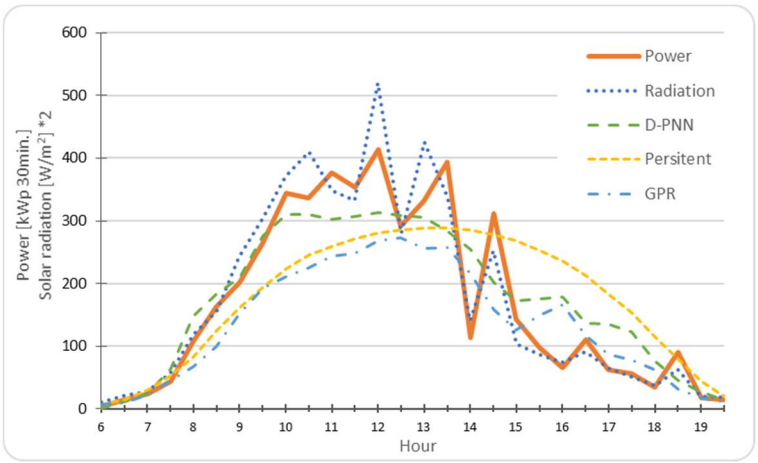

Figure 6. St. Lhota, 16 May 2011: variable cloudiness (catching and sunny periods follow); RMSE: D-PNN = 60.09; Persistent = 89.51; SMLT = 78.1 kWp 30 min.

The ratios of the averaged PVP series and the difference values show the relative involvement in the day PV patterns (Figure 7). Slight variations in the data indicate a smooth plain in PVP cycles in settled sunny weather. These phenomena are contrary to the ramping fluctuations in PVP day series, mostly in cloudy weather (Figure 6). The prediction errors in day ahead PVP estimations may be related to relative ratios and absolute differences obtained on PVP data series (Figure 7; they can denote a pattern complexity in daily PVP cycle series in consideration of the PV power average/maxima. Figure 8 presents the mean R^2 determination parameter in the prediction of PV power 24 h in advance. The models of D-PNN and SMLT better perform in case of different estimations in the optimal training data sample sequences in comparison to the benchmark reference solutions (Figure 9), i.e., the varying number of the training data records can result in analogous prediction series (Figure 8).

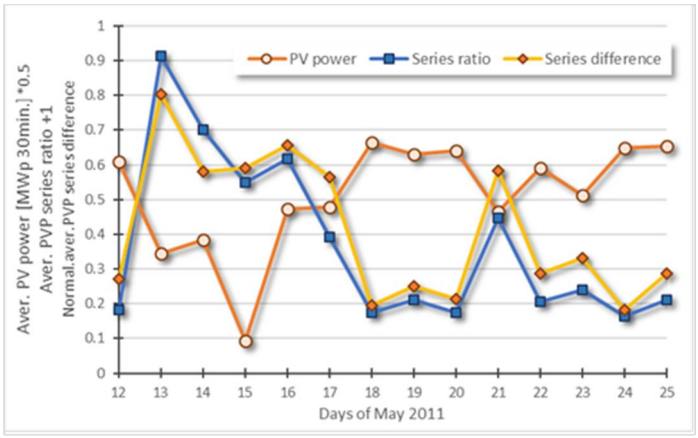

Figure 7. The daily average PV series ratios are dimensionless and characterize daily data patterns regard-less of the absolute power values, 12–25 May 2011.

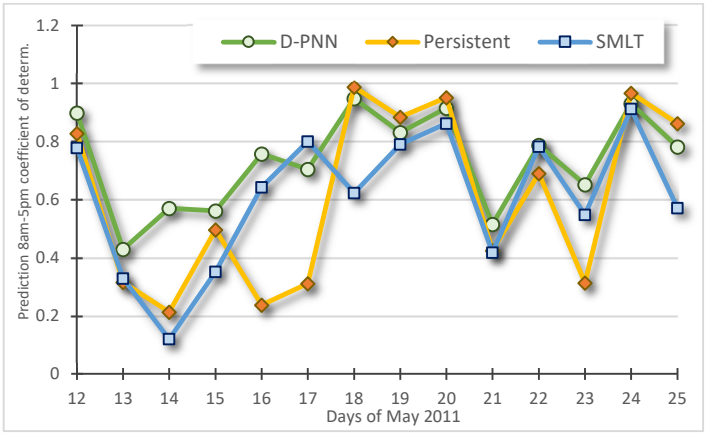

Figure 8. The 2-week daily average PVP prediction coefficient of determination R^2: D-PNN = 084, Persistent = 0.787, SMLT = 0.79.

The reference models mostly perform worse in changeable cloudy weather; however, lower errors in the 24 h persistent prediction can be obtained in days with a higher degree of similarity in patterns indicated by smooth plain PVP cycles (no ramping events). The applied AI models show slight inaccuracies in this specific condition if the last-day unsettled changeable weather intervals are suddenly broken by an overnight front, resulting in a sunny-day character (the second week in the examined data period). SMLT models obtain more accurate prediction data, as compared to D-PNN, in days of settled stable weather conditions, including a few previous days. The AI predictions can sometimes obtain an

increase in the final model accuracy in the early afternoon (Figure 6). These phenomena are directly related to particular weather patterns and characteristics of training data samples in days of forecasts. An increase in forecast errors in the first week data is related to unsettled weather conditions resulting in more complex data patterns not fully applicable to AI learning. Output errors denote the operability of finally tested prediction models in processing the reserved last observed data sequences applied on the 24 h horizon.

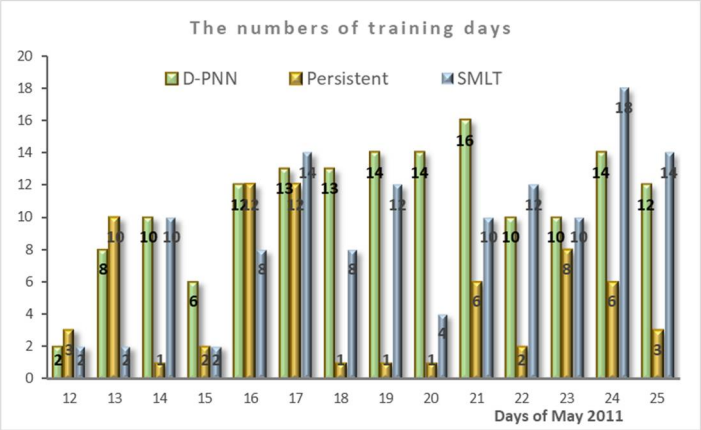

Figure 9. Daily initialization time of the 24 h PVP prediction models.

6. Conclusions

Estimated day sequence optima in the training data eliminate sudden variations and rapid changes in local weather situations. New approaches applicable in a more adequate selection of data sample records can try to recognize the frontal overnight change breaks in weather progress. The following data intervals can be applied in training, in place of the initial model identification scheme. Data patterns can be re-analyzed in a longer time interval (if available the observations) to extract adequate training data records according to the pattern similarity, one by one, in order to obtain the test error minima, not necessarily considering the sequence in the day time.

Author Contributions: Conceptualization, L.Z. and V.S.; methodology, L.Z.; software, L.Z.; validation, V.S.; formal analysis, L.Z.; investigation, V.S.; resources, V.S.; data curation, L.Z.; writing—original draft preparation, L.Z.; writing—review and editing, L.Z.; visualization, L.Z.; supervision, V.S.; project administration, V.S.; funding acquisition, V.S. All authors have read and agreed to the published version of the manuscript.

Funding: This research received no external funding.

Institutional Review Board Statement: Not applicable.

Informed Consent Statement: Not applicable.

Data Availability Statement: Data and software: https://drive.google.com/drive/folders/1ZAw8KcvDEDM-i7ifVe_hDoS35nI64-Fh.

Acknowledgments: The work was supported by SGS, VSB—Technical University of Ostrava, Czech Republic, under the grant "Parallel processing of Big Data IX" [No\SGS2022/12].

Conflicts of Interest: The authors declare no conflict of interest.

References

1. Vannitsem, S. Dynamical properties of mos forecasts: Analysis of the ecmwf operational forecasting system. *Weather. Forecast.* **2008**, *23*, 1032–1043. [CrossRef]
2. Inman, R.H.; Pedro, H.T.; Coimbra, C.F. Solar forecasting methods for renewable energy integration. *Prog. Energy Combust. Sci.* **2013**, *39*, 535–576. [CrossRef]

3. Shi, J.; Lee, W.-J.; Liu, Y.; Yang, Y.; Wang, P. Forecasting power output of photovoltaic systems based on weather classification and support vector machines. *IEEE Trans. Ind. Appl.* **2012**, *148*, 1064–1069. [CrossRef]
4. Zjavka, L.; Krömer, P.; Mišák, S.; Snášel, V. Modeling the photovoltaic output power using the differential polynomial network and evolutional fuzzy rules. *Math. Model. Anal.* **2017**, *22*, 78–94. [CrossRef]
5. Zjavka, L.; Sokol, Z. Local improvements in numerical forecasts of relative humidity using polynomial solutions of general differential equations. *Q. J. R. Meteorol. Soc.* **2018**, *144*, 780–791. [CrossRef]
6. Nikolaev, N.Y.; Iba, H. *Adaptive Learning of Polynomial Networks*; Genetic and evolutionary computation; Springer: New York, NY, USA, 2006.
7. Coimbra, C.; Kleissl, J.; Marquez, R. *Overview of Solar Forecasting Methods and a Metric for Accuracy Evaluation*; Elsevier: Amsterdam, The Netherlands, 2013; pp. 171–194.
8. Zjavka, L.; Mišák, S. Direct wind power forecasting using a polynomial decomposition of the general differential equation. *IEEE Trans. Sustain. Energy* **2018**, *9*, 1529–1539. [CrossRef]
9. Zjavka, L.; Snášel, V. Constructing ordinary sum differential equations using polynomial networks. *Inf. Sci.* **2014**, *281*, 462–477. [CrossRef]
10. Weather Underground Historical Data. Available online: https://www.wunderground.com/history/daily/LKTB/date/2016-7-22 (accessed on 24 June 2022).
11. Matlab-Statistics and Machine Learning Tool-Box for Regression. Available online: www.mathworks.com/help/stats/choose-regression-model-options.html (accessed on 24 June 2022).